Clim. Past Discuss., 9, 5479–5519, 2013
www.clim-past-discuss.net/9/5479/2013/
doi:10.5194/cpd-9-5479-2013

Climate of the Past Discussions
Open Access

The response of the Peruvian Upwelling Ecosystem to centennial-scale global change during the last two millennia

R. Salvatteci[1,2], D. Gutiérrez[2,3], D. Field[4], A. Sifeddine[1,3,5,6], L. Ortlieb[1,3,6], I. Bouloubassi[7], M. Boussafir[8], H. Boucher[1,6], and F. Cetin[1,6]

[1]LOCEAN, UMR7159 (IRD, CNRS, UPMC, MNHN), Institut Pierre Simon Laplace, Laboratoire d'Océanographie et du Climat: Expérimentations et Analyses Numériques, Centre IRD France Nord, 32 avenue Henri Varagnat, 93143, Bondy cedex, France
[2]Instituto del Mar del Perú (IMARPE), Dirección General de Investigaciones Oceanográficas y Cambio Climático, Esquina Gamarra y General Valle s/n, Callao, Perú
[3]Universidad Peruana Cayetano Heredia, Programa de Maestría en Ciencias del Mar, Av. Honorio Delgado 430, Urb. Ingeniería, S.M.P, Lima, Perú
[4]Hawaii Pacific University, College of Natural Sciences, 45-045 Kamehameha Highway, Kaneohe, Hawaii, 96744-5297, USA
[5]Departamento de Geoquimica, Universidade Federal Fluminense, Niteroi, Brasil
[6]LMI PALEOTRACES (Institut de recherche pour le développement, France; Universidade Federal Fluminense, Niteroi, Brasil; Universidad de Antofagasta, Chile)

[7]LOCEAN, UMR7159 (IRD, CNRS, UPMC, MNHN), Institut Pierre Simon Laplace, Laboratoire d'Océanographie et du Climat: Expérimentations et Analyses Numériques, Université P. et M. Curie, 4 place Jussieu, PO Box 100, 75252, Paris cedex 05, France
[8]Institut des Sciences de la Terre d'Orléans, UMR7327 INSU/CNRS/BRGM/Université d'Orléans, 1A rue de la férollerie, 45071, Orléans cedex-2, France

Received: 29 August 2013 – Accepted: 9 September 2013 – Published: 30 September 2013

Correspondence to: R. Salvatteci (renatosalvatteci@gmail.com)

Published by Copernicus Publications on behalf of the European Geosciences Union.

Abstract

The Tropical Pacific ocean-atmosphere system influences global climate on interannual, decadal, as well as at longer timescales. Given the uncertainties in the response of the Tropical Pacific to the ongoing greenhouse effect, it is important to assess the natural range of the Tropical Pacific climate variability in response to global natural changes, and to understand the underlying mechanisms. The Peruvian Upwelling Ecosystem (PUE) represents an ideal area to reconstruct past changes in ocean-atmosphere systems because productivity and subsurface oxygenation are strongly linked to changes in the strength of the Walker circulation. Throughout the last 2000 yr, warmer (the Roman Warm Period [RWP], the Medieval Climate Anomaly [MCA] and the Current Warm Period [CWP]), and colder (the Dark Ages Cold Period [DACP] and Little Ice Age [LIA]) intervals occurred with considerable changes around the globe. In order to reconstruct the PUE response to these climatic periods and reveal the underlying mechanisms, we use a multi-proxy approach including organic and inorganic proxies in finely laminated sediments retrieved off Pisco (~ 14° S), Peru. Our results indicate that the PUE exhibited a La Niña-like mean state during the warm periods, characterized by an intense OMZ and high marine productivity. During cold periods the PUE exhibited an El Niño-like mean state, characterized by a weak OMZ and low marine productivity. Comparing our results with other relevant paleoclimatic reconstructions revealed that changes in the strength of the Walker circulation and the expansion/contraction of the South Pacific Sub-tropical High controlled productivity and subsurface oxygenation in the PUE during the last two millennia. This indicate that large scale circulation changes are the driving forces in maintaining productivity and subsurface oxygenation off Peru at centennial time scales during the past two millennia.

1 Introduction

The Tropical Pacific ocean-atmosphere system influences global climate on interannual to decadal time scales (Philander, 1990; Bratcher and Giese, 2002), as well as at longer timescales with profound long-term effects (Koutavas et al., 2002; Kienast et al., 2006; Partin et al., 2007). Given the uncertainties in the response of the Tropical Pacific to the ongoing greenhouse effect (Vecchi et al., 2006; Luo et al., 2012), it is important to assess the natural range of the Tropical Pacific climate variability in response to global natural changes, and to understand the underlying mechanisms (Graham et al., 2011). Throughout the past two thousand years, periods of warmer climate (the Roman Warm Period [RWP, from ~ 50 to 400 AD], the Medieval Climate Anomaly [MCA, from ~ 900 to 1350 AD]) have alternated with colder periods (the Dark Ages Cold Period [DACP, from ~ 500 to 900 AD] and the Little Ice Age [LIA, from ~ 1500 to 1850 AD]) (Lamb, 1995; Mann et al., 2009; Graham et al., 2011). These periods have been identified in the Northern Hemisphere, but continental-scale temperature reconstructions show no globally synchronous multi-decadal warm or cold intervals that define a worldwide MCA or LIA (PAGES 2k Network, 2013). However, they show that during the past millennium, the first four centuries (1000–1400 AD) were warmer than the following four centuries (1400–1800 AD). The general long-term cooling trend ended late in the XIX century, and the last century (the Current Warm Period [CWP, from ~ 1900 to the date] was the warmest period during the past two millennia except in Antarctica (PAGES 2k Network, 2013).

The Peruvian Upwelling Ecosystem (PUE) is one of the most productive zones in the Tropical Pacific, but detailed paleoceanographic reconstructions with well-constructed age models exist only for the past 600 yr, showing large climatic, oceanographic and biogeochemical changes. The PUE represents an ideal area to reconstruct past changes in ocean-atmosphere systems, such as the Walker circulation, because productivity and subsurface oxygenation are strongly linked to changes in the strength of this atmospheric circulation at interannual timescales. Off Callao (~ 12° S) and Pisco

(~ 14° S), paleoceanographic reconstructions indicate that a dramatic reduction of export production occurred during the LIA, associated with a weak Oxygen Minimum Zone (OMZ) compared to the last ~ 100 yr (Diaz-Ochoa et al., 2008; Sifeddine et al., 2008; Gutierrez et al., 2009). The lower productivity off Peru during the LIA was associated with an increase in terrestrial input, suggesting higher precipitation in Peru, as also inferred from continental records (Reuter et al., 2009; Bird et al., 2011). The PUE response to the LIA was interpreted to be a result of a mean southward displacement of the Intertropical Convergence Zone (ITCZ) and a reduced influence of the South Pacific Sub-tropical High (SPSH) along the Peruvian margin (Sifeddine et al., 2008; Gutierrez et al., 2009).

The few paleoceanographic reconstructions off Peru covering longer time periods show conflicting climatic interpretations, most likely due to problems associated with the age models developed in each sediment core. The MCA was inferred as a relatively homogeneous period of extreme drought without strong flooding and with persistently weak El Niño activity (Rein et al., 2004). In addition, Agnihotri et al. (2008) showed that during the MCA the subsurface denitrification was lower in comparison with the start of the LIA, and that oceanographic changes during this period were of minor intensity. In contrast to the hypothesis of a relatively homogenous period during the MCA (Rein et al., 2004; Agnihotri et al., 2008), a biomarker study off Callao showed considerable differences in the El Niño activity during the MCA (Makou et al., 2010). At large, several works suggest that the MCA (LIA) was characterized by a La Niña-like (El Niño-like) mean state condition and lower El Niño (La Niña) activity (e.g., Rein et al., 2004; Sifeddine et al., 2008; Gutierrez et al., 2009; Makou et al., 2010). However, a direct comparison of different proxies from different records off Peru should be made with caution, because of chronological problems (e.g., varying reservoir ages in space and time), as well as problems with the stratigraphy of each core (Salvatteci et al., in revision). Moreover, the response of the PUE to climate changes during older periods, like the RWP and DACP, has only been assessed to a limited extent (Rein et al., 2005; Agnihotri et al., 2008).

To date there is also still a clear lack of understanding about the mechanisms controlling marine productivity in the PUE at centennial timescales. Two important mechanisms have been suggested: changes in the Walker circulation strength, and changes in the strength of the SPSH (Gutierrez et al., 2009). Hypothetically, changes in the zonal sea surface temperature (SST) gradient across the Tropical Pacific may be a principal driver for large-scale climate changes off Peru during the last two millennia given the tightly coupled system of the Western Pacific warm pool, the East Pacific cold tongue, and Walker circulation (Pierrehumbert, 2000). The large variations in the strength of the Walker circulation would suggest changes in the thermocline depth in the Eastern Pacific, with a shallower thermocline during the warm RWP and MCA and a deeper thermocline during the cold DACP and LIA. Under this scenario, the PUE should present higher productivity during the RWP and MCA compared to the cool DACP and LIA. On the other hand, changes in the strength of the SPSH could also be responsible for changes in the PUE since this atmospheric circulation regulates the strength of the alongshore winds off Peru (Aceituno et al., 1993). The southern rim of the SPSH has shifted during the last two millennia, suggesting an expansion of the SPSH during the RWP and MCA, producing stronger alongshore winds, and a contraction during the cold DACP and cool LIA (Lamy et al., 2001). Accordingly, we would expect higher marine productivity off Peru during the warm RWP and MCA. The opposite is expected for the cold DACP and cool LIA. The relationship between wind strength and marine productivity is not that straightforward though, since the thermocline/nutricline depth plays a major role; a deep thermocline/nutricline in combination with stronger alongshore winds will likely produce non-productive upwelling. Paleoceanographic reconstructions in the Eastern Pacific during the last two millennia are needed to assess the response of the PUE to the zonal SST gradient and the role of the SPSH modulating the oceanographic variability in this area.

In the present study, for the first time, we elucidate the response of the PUE to centennial scale changes in the strength of the Walker circulation and the expansion/contraction of the SPSH. For this, we use a multi-proxy approach including or-

ganic and inorganic proxies in finely laminated sediments retrieved off Peru. This area is strongly influenced by both ENSO/Walker circulation (Philander, 1990), and by centennial climate variability (Agnihotri et al., 2008; Sifeddine et al., 2008; Chazen et al., 2009; Gutierrez et al., 2009). We reconstruct key aspects of the PUE: productivity and OMZ intensity, both of them strongly linked to changes in the strength of the Walker circulation through changes in the thermocline depth. First, we reconstruct the terrigenous input, to assess if terrigenous contents in the cores are concordant with the ITCZ displacements over the continent. During the MCA, the ITCZ was in a more northern position than during the LIA (Haug et al., 2001), thus it is expected that the PUE presents a contrasting behavior in the two periods if the ITCZ displacement was the dominant factor. Next, the intensity of the OMZ was reconstructed as it fuels the euphotic layer with nutrients, and also because a strong OMZ may limit the habitat of several pelagic organisms (Stramma et al., 2010; Bertrand et al., 2011). The OMZ intensity may be regulated by remote forces (changes in ventilation and/or water masses) or by local productivity (Pennington et al., 2010). If the remote ventilation of the OMZ dominates over the local productivity we expect the water column oxygenation not to be coupled with the inferred local productivity. On the contrary, if the local productivity dominates the oxygen demand, then the subsurface conditions and the export production are expected to be closely related. Additionally, we reconstruct oxygen availability in the sediments because a decoupling between the oxygen content in the water column and the sediments may imply changes in the circulation pattern of bottom water masses. Finally, two different types of export production are reconstructed: siliceous productivity and overall export production, which includes export production from higher trophic levels.

The objectives of this work are twofold: first, we set out to define the centennial mean state (El Niño/La Niña-like) of the PUE in contrasting (warm and cool) periods, such as the RWP, DACP, MCA, LIA and CWP. At interannual timescales, a reduction of the Walker circulation during El Niño events results in an increase in sub-surface oxygenation and reduced productivity off Peru due to a deepening of the thermocline,

whereas the opposite is the case for La Niña events. Following the observed changes at interannual timescales, the multidecadal to centennial-scale periods with higher (lower) export production and strong (weak) OMZ conditions are interpreted in the present work to represent persistent La Niña (El Niño)-like conditions. Second, the results of the present work are compared with records of changes in Walker circulation strength and SPSH expansion/contraction to assess the influence of changes in these systems over the PUE. Therefore, we compare our results with relevant paleoclimatic reconstructions in the Tropical Pacific to understand the mechanisms that controlled the productivity and OMZ intensity off Peru during the last two millennia.

2 Environmental setting

2.1 Characteristics of the Peruvian Upwelling Ecosystem

The PUE is an eastern boundary upwelling system characterized by a shallow surface mixed layer, a shallow thermocline and high productivity driven by coastal upwelling of nutrient-rich cold waters that are poorly ventilated (Barber and Chavez, 1983; Pennington et al., 2006). In the PUE the seasonal production cycles are out of phase with seasonal increases in upwelling winds, in clear contrast to the other eastern boundary upwelling systems (Pennington et al., 2006; Chavez and Messié, 2009). Upwelling favorable winds occur during the entire year but are stronger during austral winter and spring (Strub et al., 1998; Echevin et al., 2008). By contrast, primary productivity is higher during austral spring and summer when surface waters are more stratified (Pennington et al., 2006; Chavez and Messié, 2009). The seasonal variability of the mixed layer depth is the main controlling factor of the primary productivity seasonality (Echevin et al., 2008). In austral winter, the mixed layer deepening reduces the concentration of chlorophyll because of a dilution effect and light limitation, while during the austral summer the primary producers concentrate near the surface in the shallow mixed layer and nitrate limitation occurs (Echevin et al., 2008). The seasonal

changes in winds and productivity in the PUE are associated with the meridional displacement of the eastern SPSH from ∼32° S in austral summer to ∼28° S in austral winter (Karstensen and Ulloa, 2009). The ITCZ also shows a seasonal latitudinal displacement from 2–5° N in austral summer to 10° N in austral winter (Fig. 1; Strub et al., 1998).

The upwelling intensity is not the only factor that maintains productivity in the PUE, but also the supply of nutrient-rich and oxygen-poor waters to the region via the Poleward Undercurrent located between ∼50 to >400 m depth (Karstensen and Ulloa, 2009). As a combination of lack of ventilation, long residence times and the decay of biological production that consumes O_2, a strong and shallow OMZ is present off Peru intersecting the upper continental margin from ∼50 to 600 m depth (Helly and Levin, 2004; Pennington et al., 2006). This strong OMZ inhibits bioturbation and preserves sediments containing millimeter-scale laminae that permit to reconstruct past ecosystem changes at high resolution levels (Gutierrez et al., 2006). The Poleward Undercurrent is fed from the Equatorial Current System by the Equatorial Undercurrent and by Southern Subsurface Countercurrents, and also by alongshore recirculation and from currents located south of ∼9° S (Montes et al., 2010). Consequently, temporal changes in the intensity and ventilation of these currents can affect the oxygen and nutrient availability in the Poleward Undercurrent that ultimately fuels the euphotic layer via upwelling.

Reconstructions of the PUE extending to the last two millennia suffer from chronological problems as well as problems with the stratigraphy, and lack accurate age model constructions due to varying reservoir ages in space and time. Consequently, the response of the PUE to centennial scale global change is not completely understood because of the lack of a widely accepted archival record. The reasons for the non-continuous nature of the sedimentary marine record off central Peru are repeated bioturbation events, erosion by bottom currents (Reinhardt et al., 2002), and slumps due to seismic activity (Salvatteci et al., 2013). The numerous discontinuities and slumped/ homogeneous sections imply that a cautious and precise core stratigraphy

must be developed before any climatic interpretations can be proposed (Salvatteci et al., 2013). For example, overlooking a hiatus may erroneously lead to infer abrupt climate changes, and slumped sections may be interpreted as periods with low climatic variability (Salvatteci et al., 2013). These problems with the sedimentary column are even more relevant for studies focusing on reconstructions at high resolution (e.g., Rein et al., 2004, 2005; Agnihotri et al., 2008).

2.2 Changes in ocean-atmosphere systems as a driver for changes in the PUE during the last two millennia

Changes in the SST gradient across the Tropical Pacific (i.e. zonal SST gradient) could be a principal driver for large-scale climate changes off Peru during the last two millennia. This zonal SST gradient, between the Tropical Indo-Pacific warm pool in the west and the Central/Eastern Tropical Pacific, is dependent on variations in total solar irradiation, resulting in circulation changes driving climate shifts around the planet (Mann et al., 2009; Graham et al., 2011). According to this "thermostat mechanism", increased solar irradiance tends to intensify the east-west temperature gradient, which strengthens the equatorial easterlies and increases the upwelling in the equatorial Pacific, amplifying the thermocline tilt towards the east (Clement et al., 1996). The SST asymmetry between the warm Eastern Pacific and cold Eastern Equatorial Pacific is the principal factor controlling the intensity of the Walker Circulation along the equator (Bjerknes, 1969). Moreover, the latitudinal position of the ITCZ contributes to the modification of the zonal SST gradient by the expansion/contraction of the Southeast Pacific cold tongue (Koutavas and Lynch-Stieglitz, 2005). Changes in the SST zonal gradient and thus the Walker circulation strength, and the ITCZ during the last two millennia, suggest a stronger (weaker) Walker circulation during the MCA (LIA), inducing La Niña (El Niño)-like mean state (Cobb et al., 2003; Mann et al., 2005, 2009; Oppo et al., 2009; Conroy et al., 2009, 2010).

Another factor that influences large-scale climate changes off Peru is the expansion/contraction of the SPSH. This atmospheric circulation regulates the strength of

the alongshore winds off Peru, forcing the upwelling of subsurface nutrient rich waters along the Peruvian coast (Aceituno et al., 1993; Strub et al., 1998). The southern rim of the SPSH also experienced important meridional displacements during the last two millennia as inferred from the meridional changes in the position of the Southern Westerlies off Chile (Lamy et al., 2001; Mohtadi et al., 2007; Moy et al., 2009), indicating changes in the expansion/contraction of the SPSH. According to this, the SPSH contracted during the cold periods (DACP and LIA) and expanded during the RWP and part of the MCA (Lamy et al., 2001). In addition, a dust particle dataset from the West Antarctica Ice Sheet also indicates that the southern Westerlies were stronger and occupied a more southerly position during part of the MCA (~ 1050 to 1430 AD), and that the Westerlies were weaker and occupied a more equatorward position during almost the entire LIA (1430–1950 AD; Koffman et al., 2013).

3 Material and methods

3.1 Sampling site and cores used in the present study

Nine gravity and box-cores were selected from more than 30 cores to determine the continuity of the records and to select the best records (SM1; Salvatteci et al., 2013). All cores were retrieved off Pisco, Peru (Fig. 1), because this area presents finely laminated sequences allowing high-resolution reconstructions (SM1). Given the problems with the sedimentary column continuity (Salvatteci et al., 2013), we applied a detailed stratigraphic approach to construct an accurate age model (SM1 and SM2). After a careful revision of sedimentary characteristics, we selected box-core B0506-14 (hereafter B-14) retrieved at 301 m depth (14.27° S, 76.43° W; Fig. 1) for the present study as it presented the most continuous, undisturbed and well-preserved laminae sequences (SM1). The presence of small-scale discontinuities and mixed sequences present in B-14 (Salvatteci et al., in revision) do not affect the centennial scale changes of the proxy records that are the focus of the present work. Core B-14 covers approximately

the last ~ 500 yr, but in order to infer changes prior to the LIA, we analyzed a laminated section from a 5.2 m long gravity core (G-10), whose upper part overlaps with core B-14 bottom (SM1). Core G-10 was retrieved during the Galathea-3 expedition in 2007 at 312 m depth (14°23 S, 76°23.9 W) near the B-14 location (Fig. 1).

For a detailed description of the two cores used in this work, the stratigraphic approach, the subsampling procedure, the composition of the assembled core, and the development of the age model, we refer to the Supplement SM1, SM2 and SM3.

3.2 Rationale behind the choice of proxies

3.2.1 Terrigenous input

The terrigenous input was inferred from Aluminum (Al) and Titanium (Ti) contents. The terrigenous material in the shelf is principally delivered by rivers that dilute the terrigenous components of eolian origin (Scheidegger and Krissek, 1982) and thus can be used as a proxy of fluvial discharge.

3.2.2 Redox conditions

In order to reconstruct sediment redox conditions we used a series of trace elements that exhibit different sensitivities to redox conditions such as Molybdenum (Mo), Vanadium (V) and Rhenium (Re), and may permit the differentiation between anoxic (sulfate reducing) or suboxic ($0.2 > [O_2] > 0$ ml L^{-1} and no H_2S) conditions at the time of deposition. Additionally, Mo, V, and Re are heavily enriched in OMZ sediments off Peru, have minimal detrital influence, and display a conservative behavior in the water column (Colodner et al., 1993; Böning et al., 2004; Tribovillard et al., 2006). Molybdenum is enriched mainly under anoxic, sulfate-reducing conditions, when H_2S is available (Crusius et al., 1996; McManus et al., 2006; Tribovillard et al., 2006). Vanadium is reduced and accumulates under denitrifying conditions but also under more strongly reducing (i.e. anoxic) conditions. Re concentrations in the continental crust and in the seawater are

extremely low but are strongly elevated in reducing sediments with absence of O_2 and H_2S (Crusius et al., 1996; Böning et al., 2004), but also (perhaps to a lesser extent) in sulfidic sediments (Crusius et al., 1996). Mo, V, and Re accumulate via diffusion across the sediment-water interface according to the extent of reducing conditions (Böning et al., 2004; Tribovillard et al., 2006). Thus, sediments exhibiting concurrent enrichments in V, Re and Mo reflect euxinic conditions ($[O_2] = 0$; presence of H_2S) at the sediment water interface whereas an enrichment of Re (and also V to a lesser extent) without Mo enrichment reflects suboxic (absence of H_2S) conditions (Tribovillard et al., 2006).

3.2.3 Export production

In order to infer export production we use a set of trace metals, TOC, and biogenic silica contents that represent different types of productivity. Nickel (Ni), Copper (Cu) and Cadmium (Cd) are expected to represent export production because they display a nutrient-like behavior in the water column, are present in considerable concentrations in plankton, and it seems that the dominant source of these elements is bio-detritus (Böning et al., 2004; Nameroff et al., 2004; Dean et al., 2006; Tribovillard et al., 2006). Ni, Cu and Cd are frequently used as proxies of the original presence of organic matter (OM); these elements are delivered to the sediments in association with OM, fixed in the sediments under reducing conditions and are moderately enriched in sediments off Peru (Böning et al., 2004; Dean et al., 2006; Tribovillard et al., 2006). Cd is heavily enriched in marine sediments off Peru (Böning et al., 2004). Total Organic Carbon (TOC) was also analyzed to reconstruct export production and to examine the relationship with the productivity proxies. Ni, Cu, Cd, and TOC should reflect the export production from the euphotic zone that escapes remineralization in the upper meters of the water column. This export production is basically composed by large particles like fecal pellets or large marine snow (Suess, 1980), and is not a simple function of productivity since is highly dependent on the pelagic community structure and trophic pathways (Michaels and Silver, 1988; Rodier and Le Borgne, 1997), thus also representing biomass variability of higher trophic levels. Finally, biogenic silica contents were also analyzed in

order to infer primary production exclusively originated from siliceous biota such as diatoms, radiolaria, siliceous sponges, and silicoflagellates (DeMaster, 1981).

3.2.4 Water column denitrification

$\delta^{15}N$ records from sedimentary OM is taken as a proxy of water-column denitrification in oxygen-deficient waters (Altabet and Francois, 1994; Altabet et al., 1999; De Pol-Holz et al., 2006; Martinez and Robinson, 2010; Mollier-Vogel et al., 2012), and generally reflects regional to large-scale changes. In oxygen-deficient waters, bacteria reduce nitrate to N_2, leaving the remaining nitrate pool enriched in ^{15}N which is transferred by upwelling to the surface, where it is used by phytoplankton and ultimately transferred to the sediments (Altabet and Francois, 1994; Agnihotri et al., 2008). However several other factors can contribute to the $\delta^{15}N$ signal in the sedimentary organic matter, like N_2 fixation by diazotrophic bacteria, nitrification, the extent of surface NO_3^- utilization, and the anammox reaction (Robinson et al., 2012). Nevertheless the sedimentary $\delta^{15}N$ signal off Peru is consistent with other proxies of oxygenation and productivity implying denitrification in the water column at least during the last millennia (Agnihotri et al., 2008; Gutierrez et al., 2009).

For a detailed description of the analytical procedures of each element, we refer to Supplement SM4.

3.3 Statistical procedures

To establish the relationships among the different proxies, we calculated the Pearson correlation coefficients (r) using the Statistica software (Statsoft, 2005). The probability level was corrected for multiple comparisons by dividing the probability level α ($p < 0.05$) by the number of tests performed (Glantz, 2002). Given that 12 test were performed, the corrected probability level was $p < 0.0042$.

4 Results

4.1 Proxy relationships and data presentation

Proxies representing the same processes are mostly highly correlated with exception of Cd, which seems to follow sediment redox conditions instead of export production (SM6 and SM7). The relationships among proxies for sediment redox conditions show an expected behavior due to their sensitivity to sediment oxygen levels: Mo and Re are negatively correlated, while the relationship between Mo and V is stronger than that between Re and V. Water column denitrification (δ^{15}N) was highly correlated with oxygen contents in the sediments as inferred by Mo and Re / Mo. Some relationships among proxies for export production were highly correlated with other productivity proxies whereas others not; these observations can be used to interpret changes in productivity during the last two millennia. Biogenic silica contents show negative correlations with the other export production proxies indicating that the overall export production (i.e. from higher trophic levels) is not a simple function of siliceous productivity, but rather depends on oceanographic conditions or might be influenced by post-depositional processes. There are generally higher correlations between TOC, Ni, and Cu than between these and Cd, suggesting that TOC, Ni, and Cu may be better indicators of export production. Moreover the correlations between Cd and the sediment redox conditions (Mo and V) are stronger than the correlations between Cd and the export production proxies (TOC, Ni, Cu) suggesting that Cd may be a better indicator of sediment redox conditions than export production. Finally, biogenic silica is strongly correlated with water column denitrification whereas the other export production proxies show relatively weak correlations. For the detailed correlation values, we refer to Supplement SM7 and SM10.

We present the standardized authigenic concentrations of the trace elements in Fig. 2 instead of the Al normalization or metal accumulation rates. Normalization of trace elements concentrations through division by Al as well as the calculation of fluxes (Metal concentration x sedimentation rates x DBD) through the use of the sedimentation rates obtained from age models, are common practices. However, in the present dataset, the normalization procedure increased, decreased, or even changed the sign of the correlations between unmodified variables (SM8). The large variations in the sedimentation rates (SM3) also produced distorted correlations between elements (data not shown). Consequently, we present the authigenic concentrations of the trace elements instead of metal fluxes or Al normalization. Nonetheless, the average enrichment factor of each element in the whole record was calculated to determine which elements exhibit the highest enrichments relative to andesite (SM9, SM10). The high and moderate enrichment factors of Re, Cd, Mo, Ni, and V support their use as paleoredox or paleoproductivity proxies.

The differences in the sedimentation rates (between periods) and the different subsampling thickness (between cores) indicate that the average time span of each sampled interval during the RWP, DACP, MCA, LIA and CWP is 21.9, 21.9, 7.5 and 1.1 yr respectively. Consequently, the proxies obtained in the samples corresponding to the LIA and CWP periods were lumped in intervals of approximately 20 yr, and the results are presented as standardized values (value-average / sd).

4.2 Terrigenous input

The terrestrial runoff proxies indicate drier conditions during the last stage of the MCA (~ 1170 to 1350 AD) and the last 150 yr, and more humid conditions during the cold periods and during part of the MCA (Fig. 2a and b). The most humid conditions are recorded during the cold DACP and from ~ 1050 to 1170 AD during the MCA. The MCA in our record shows two periods with strong differences in terrestrial input, a period with high values from ~ 1050 to 1170 AD and a period with low values from ~ 1170 to 1350 AD. The cold LIA shows more humid conditions in comparison with the dry stage of the MCA and the last 150 yr. During the LIA, from ~ 1550 to 1750 AD, reduced terrigenous input is recorded in comparison with the start and end of this period, but the values are still higher in comparison with the last stage of the MCA and during the CWP. The transition from the MCA to the LIA shows a gradual increase in terrestrial

input, while the transition from the LIA to the CWP shows an abrupt decrease as also reported by Sifeddine et al. (2008) and Gutierrez et al. (2009).

4.3 Water column oxygenation and sediment redox conditions

Water column denitrification and the sedimentary redox conditions, particularly Mo and Re / Mo, are strongly coupled throughout the record implying low influence of remote oxygenated bottom waters (e.g., Antarctic Intermediate Water) that could be responsible for the decoupling between water column and sediment oxygenation (Fig. 2c–h). The δ^{15}N profile shows large centennial scale changes suggesting less water column denitrification and hence a weaker OMZ during the cold DACP and LIA, and more intense water column denitrification and OMZ during the warmer MCA and CWP (Fig. 2c). Authigenic Mo, V and Cd contents and particularly the Re / Mo indicate less authigenic enrichment (sub-oxic conditions) during the cold periods (DACP and LIA), and more authigenic enrichment (anoxic conditions) during part of the RWP, the last stage of the MCA, and from the end of the LIA to the present (Fig. 2c–h), which is consistent with the changes in water column oxygenation.

The Re / Mo ratio, that serves to differentiate anoxic (with available H_2S) conditions and sub-oxic conditions, is higher during the cold DACP and LIA, giving support to the dominance of suboxic conditions in the surface sediments (Fig. 2h). By contrast, during the last stage of the MCA (1170 to 1350 AD) and from the end of the LIA until 2005, the Re / Mo values were close to or below 0.4×10^{-3} (dashed line in Fig. 2h), indicating predominant anoxic conditions. The inferred oxygenation in the water column and in the sediments was higher during the cold LIA in comparison with the cool DACP (Fig. 2c–h).

A closer look into the MCA reveals two different stages with contrasting characteristics in the oxygen content in the sediment-water interface and the water column (Fig. 2c–h). From ∼ 1050 to ∼ 1170 AD, higher Re / Mo values and relatively lower δ^{15}N values are consistent with sub-oxic conditions in the sediment-water interface and a relatively more ventilated water column (but these changes were less intense in com-

parison to the changes observed during the cool DACP and the cold LIA). By contrast, from ∼ 1170 AD to 1350 AD, there is a concurrent increase in Mo, very low values of Re / Mo (ratios near to 0.4×10^{-3}), and higher δ^{15}N, that indicate anoxic conditions in the sediment-water interface and an intense OMZ. The two different stages further indicate that the MCA is not a homogeneous period in the region, as also observed in the terrigenous input record, and that it is characterized by strong multi-decadal variability in oxygen content in the sediment-water interface and in the water column.

The transitions from cold to warm periods show different patterns of oxygenation change than the transitions from warm to cold periods. The RWP-DACP and MCA-LIA transitions show a gradual change from anoxic to sub-oxic conditions while the LIA-CWP transition show an abrupt change from sub-oxic to anoxic conditions (Fig. 2h). The RWP-DACP and MCA-LIA transitions, which are associated with an increase in terrestrial input (Fig. 2a and b), are characterized first by a decrease in Mo and then by a decrease in V (Fig. 2d, e and g), as expected due to the behavior of these elements to a gradual change from anoxic (available H_2S) to suboxic conditions. The δ^{15}N and Re / Mo profiles also confirm this gradual pattern implying that the change in conditions from anoxic to suboxic was gradual in the water column and in the sediments (Fig. 2c and h). By contrast, the LIA-CWP transition was characterized by an abrupt change from sub-oxic to anoxic conditions as evidenced by the Re / Mo ratio that reached a value of $\sim 0.4 \times 10^{-3}$ decades before the end of the LIA (Fig. 2h). The present day anoxic conditions in the sediments were established towards the end of the LIA. Remarkably, the gradual change from anoxic to suboxic conditions occurred when the terrestrial input was increasing, while the change from sub-oxic to anoxic conditions was reached when the terrigenous input was still high (Fig. 2a–h).

4.4 Paleoproductivity proxies

At centennial to multi-centennial timescales export production, represented both by biogenic silica and the overall export production proxies (TOC, Ni and Cu), is higher during the warm MCA and CWP and lower during the cool DACP and LIA. However,

biogenic silica and the overall export production proxies seem to be out of phase during the warm periods. Siliceous productivity is higher during the warm RWP, the last stage of the MCA, and from the end of the LIA to ~1900 AD, while it is low during the first part of the MCA, the cool DACP, the cold LIA and the last decades (Fig. 2i). TOC, Ni, and Cu authigenic contents show similar centennial-scale variability (Fig. 2j–l), with high values during NH warm periods (RWP and MCA) and the CWP, and low values during NH cold periods (DACP and LIA). During the MCA from ~1050 to 1170 AD low biogenic silica contents occur with higher overall export production proxies; by contrast, from ~1170 to 1350 AD biogenic silica increase while the other productivity proxies decrease (Fig. 2i–l). From the end of the LIA towards the present a decline in biogenic silica is also associated with an increase in the overall export production proxies. Consistent with the proxies for oxygenation, all paleoproductivity proxies show a gradual decrease during the MCA-LIA transition; however the start of the decrease pattern is different in the biogenic silica and the other productivity records (Fig. 2i–l). During the LIA-CWP transition, only the biogenic silica contents show an abrupt increase while the proxies for overall export production show a more gradual increase.

Water column and sediment oxygenation show a stronger relationship with siliceous productivity than with the overall export production proxies, indicating that siliceous productivity and the subsequent sinking and decaying have a higher contribution in the subsurface oxygen deficit (Fig. 2). The biogenic silica contents show higher relationships with proxies related to oxygenation in the water column as δ^{15}N (SM7; 0.75), and in the sediments as inferred by the Mo and Re / Mo (SM7; 0.50 and −0.58 respectively). The higher relationships with the subsurface oxygenation compared to the anoxic conditions in the sediments imply that the biogenic silica record reflects the export of primary productivity and not a preservation signal regulated by the anoxic conditions in the seafloor given that the latter is the principal factor regulating the preservation of biogenic silica in the sediments. The highest values of biogenic silica during the MCA (from ~1170 to ~1350 AD) coincide with a strong water column denitrification and an

anoxic episode in the sediments as recorded by the δ^{15}N and the Re / Mo ratio (Fig. 2c and h).

In contrast with the relationships between biogenic silica and the proxies for oxygenation, relationships of Ni, Cu and TOC with δ^{15}N are negative and weak, while the relationship with sediment redox conditions (Mo and Re / Mo) are very weak (SM7). During the MCA and the CWP the proxies for overall export production show higher values when the OMZ is less intense (Fig. 2c and 2j–l) suggesting a possible control of the overall export producers by changes in the OMZ intensity. The highest values of the overall export production proxies (Ni, Cu and TOC) prior to the CWP occurred during the MCA-LIA transition (at ~1400 AD), 100 yr after a period characterized by a strong OMZ (Fig. 2c), and when the trend towards less intense OMZ and more sub-oxic conditions in the sediments had already started (Fig. 2c and h). During the LIA-CWP transition, the highest values of Ni, Cu and TOC (Fig. 2j–l) occurred some decades after the period characterized by the strongest water column denitrification and the settlement of anoxic conditions on the seafloor (Fig. 2c and h).

5 Discussion

In the present study we define, for the first time, the mean state of the PUE in contrasting climatic periods at centennial time scales during the past two millennia: the Roman Warm Period (RWP), the Dark Ages Cold Period (DACP), the Medieval Climate Anomaly (MCA), the Little Ice Age (LIA), and the Current Warm Period (CWP). The principal results of the present study are: (1) drier conditions during the last stage of the MCA (~1170 to 1350 AD) and the past 150 yr, and more humid conditions in the cold periods and from ~1050 to 1170 AD during the MCA (Fig. 2a and b); (2) a strong OMZ and high productivity during the warm periods, whereas during the cold periods we observe a weak OMZ and low productivity (Fig. 2); (3) a strong coupling between OMZ intensity and primary productivity; (4) a gradual change from stronger to weaker OMZ, and from high to low primary productivity during the RWP-DACP and

MCA-LIA transitions, and an abrupt change from weaker to stronger OMZ, and from low to high primary productivity during the LIA-CWP transition. In the following sections we discuss ITCZ displacements inferred from the detrital contents in our records. Further, we evaluate the influence of changes in Walker Circulation strength and the SPSH expansion/contraction on the productivity and OMZ intensity off Peru during the last two millennia. For this, we compare the results of the present work with other precipitation records and selected paleoceanographic reconstructions in the Tropical and Sub-Tropical Pacific.

5.1 Terrigenous input in the Peruvian margin indicates latitudinal ITCZ displacement

The results of the present study indicate important changes in detrital contents on the Peruvian continental margin, reflecting precipitation changes over the continent, indicating major meridional ITCZ variability (Fig. 3). According to precipitation proxies over the continent (Haug et al., 2001) and in the central Pacific Ocean (Sachs et al., 2009), as well as modeling experiments (Chiang and Bitz, 2005; Broccoli et al., 2006), the ITCZ exhibited large latitudinal changes throughout the last two millennia, associated with changes in the Northern Hemisphere temperature, migrating to the north (south) during warm (cold) periods (Fig. 3a–c). These latitudinal changes in the position of the ITCZ, associated with lower precipitation in Peru during the MCA compared to the LIA, were also registered in a speleothem record from northeastern Peru (Fig. 3d), and in a varved lake in the Central Peruvian Andes (Pumacocha lake, $\sim 10.7^{\circ}$ S; Fig. 3e). Both continental records show increased precipitation during the LIA in comparison to the MCA and the past 150 yr. The terrestrial runoff proxy obtained in the present study (Pisco; Fig. 3f) is concordant with the reconstructed precipitation over the continent from the start of the MCA to the date.

The terrestrial input recorded in the present study (Fig. 3f) shows a strong multidecadal variation during the MCA that is similar to the rainfall reconstruction from continental records in Peru (Fig. 3d, Reuter et al., 2009; Fig. 3e, Bird et al., 2011). The

results of the present study as well as other precipitation records in Peru (Reuter et al., 2009; Bird et al., 2011) contradict a hitherto widely accepted record of terrestrial run-off studied in Callao, Peru (Rein et al., 2004, 2005), but are consistent with regional records of ITCZ displacements (Fig. 3g; Haug et al., 2001; Sachs et al., 2009). Rein et al. (2004, 2005) interpreted a period between ~ 750 to ~ 1250 AD (in part coinciding with the MCA period) as a dry period in Peru, based on reduced lithic contents in a marine sediment core retrieved off Callao ($\sim 12^{\circ}$ S). The radiochronological differences between the Pisco (present study) and Callao (Rein et al., 2004, 2005) records may be partly related to different delta-R estimates. More likely, the differences in the nature of the MCA in the Pisco and Callao record may be explained by stratigraphic problems not identified in the Callao core. Missing sequences and slumped deposits are a common feature in cores retrieved off Peru (Salvatteci et al., 2013). A slumped or homogeneous section could be erroneously interpreted as a period of low climate variability (Salvatteci et al., 2013), consequently overlooking these stratigraphic features leads to erroneous interpretations. On the other hand, our results clearly show that if a good chronological framework is developed, marine sediments of the continental margin reliably serve to reconstruct past precipitation changes. Another possible explanation for the discrepancy to the Rein et al. (2004, 2005) record may be related to the use of the reflectance spectra as an indicator of lithic contents. The present study, in accordance with other lines of evidence (Bradley, 2000; Bradley et al., 2003; Graham et al., 2011), indicates that the MCA in the Eastern Tropical Pacific was characterized by a range of temperatures, hydroclimate and marine changes rather than a homogeneous period with severe drought as interpreted by Rein et al. (2004).

5.2 Peruvian Upwelling Ecosystem response to ocean-atmosphere changes during the last two millennia

Our results show that during the cold periods (DACP and LIA), the PUE exhibits El Niño-like conditions with low export production (Fig. 4g and h), a weak OMZ (Fig. 4e) and sub-oxic conditions in the sediments (Fig. 4f). These features coincide with a weak

Walker circulation (Fig. 4b, Oppo et al., 2009; Fig. 4c, Conroy et al., 2009) and a SPSH contraction (Fig. 4d, Lamy et al., 2001). The weak Walker circulation suggests a deep thermocline, and a SPSH contraction likely produced weaker alongshore winds off Peru. The cold periods are also characterized by a weak OMZ and thus a deep oxycline (Fig. 4e). Consequently, the weak upwelling of nutrient-poor waters resulted in insufficient fertilization of the upper section of the water column hampering the development of primary producers (Fig. 4g). As a consequence of low primary productivity, the productivity from higher trophic levels was low as well (Fig. 4h). The climatic and oceanographic conditions were more extreme during the LIA compared to the DACP, which is also reflected by the productivity from higher trophic levels during the LIA, which is the lowest of the whole record (Fig. 4h). In contrast to the results of the present study, modern observational data, at annual or decadal timescales, suggest increased productivity in the eastern Pacific during cool periods (Chavez et al., 2011). This apparent contradiction, however, is most likely due to the different forcings responsible for cold periods at different time scales.

During the warm periods (RWP and MCA), the PUE exhibited La Niña like conditions with generally high export production (Fig. 4g and h), a strong OMZ (Fig. 4e) and anoxic sediment conditions (Fig. 4f). These features coincide with a stronger Walker circulation (Fig. 4b, Oppo et al., 2009; Fig. 4c, Conroy et al., 2009) and a SPSH expansion (Fig. 4d, Lamy et al., 2001). The strong Walker circulation suggests a shallower thermocline, and an expansion of the SPSH likely produced stronger alongshore winds off Peru. The inferred high productivity and strong OMZ during the warm periods match with the "ocean thermostat mechanism" proposed by Clement et al. (1996), suggesting that changes in solar irradiance produce changes in the thermocline depth in the eastern Pacific through changes in the Walker circulation strength. As a consequence of a stronger Walker circulation and a shallower oxycline, the upwelling from nutrient rich waters resulted in high primary productivity (Fig. 4g). Both types of export production proxies (Fig. 4g and h) show in general higher values during the MCA compared to the RWP, indicating that the climatic and oceanographic conditions during the warmer

MCA were more favorable for productivity off Peru. The clear association of marine productivity and OMZ intensity with changes in ocean-atmosphere systems shows that large scale circulation changes are the driving forces in maintaining productivity and subsurface oxygenation off Peru at centennial time scales during the past two millennia.

Our data demonstrate a strong multidecadal variability of marine productivity and subsurface oxygenation during the MCA associated with changes in the expansion/contraction of the SPSH, whereas the Walker circulation seems to be strong but relatively stable during the entire MCA. From ~1000 to 1150 AD, relatively low primary productivity and a relatively weak OMZ are observed coinciding with a stronger Walker circulation (Fig. 4b, Oppo et al., 2009; Fig. 4c, Conroy et al., 2009) and a SPSH expansion (Fig. 4d, Lamy et al., 2001). This suggests that a contraction of the SPSH produced weaker alongshore winds, producing weaker upwelling, lowering the fertilization of the upper water column, and thus producing a relatively low primary productivity even if the Walker circulation was strong (Fig. 4b and c). By contrast, during the last stage of the MCA (~1150 to ~1350 AD), the primary productivity was high, associated with a strong Walker circulation and an expansion of the SPSH. These conditions may have supported a shallower thermocline and a more stratified water column favoring the productivity in the PUE (Fig. 4). These results indicate that during the warm periods the contraction/expansion of the SPSH is more important in regulating marine productivity in the PUE than the Walker circulation, as it regulates the strength of alongshore winds that fuels the upper layers of the water column.

Whereas overall export production was strongly influenced by changes in the zonal SST gradient and the expansion/contraction of the SPSH, changes in OMZ intensity may also be an important factor regulating the productivity of higher trophic levels. The last stage of the MCA and the LIA-CWP transition were characterized by a high primary productivity (Fig. 4g) but a low overall export production (Fig. 4h) coinciding with a strong OMZ, and thus a shallower oxycline (Fig. 4e). The oxygen deficit in the water column and especially the shallower oxycline may have resulted in a reduced habitat for several pelagic organisms (Stramma et al., 2010; Bertrand et al., 2011), diminishing

their abundance and thus permitting an increase in primary producers through lower grazing pressure.

The past 100 yr are characterized by a strong OMZ (Fig. 4e) and in general high productivity (Fig. 4g and h) in accordance with former warm periods (RWP and MCA). The overall export production shows a positive trend (Fig. 4h) that could be produced by an increase in upwelling favorable winds (Gutierrez et al., 2011). Instrumental observations indicate that the Walker circulation and the SPSH experienced important changes during the last decades and may have induced changes in the PUE similar to former warm periods; the westerlies have strengthened and shifted poleward (Toggweiler, 2009; Lee and Feldstein, 2013), while the SPSH has also strengthened, possibly in response to global warming (Falvey and Garreaud, 2009). Moreover, recent observations indicate that the Tropical Pacific trade winds have strengthened over the past two decades and likely contributed to the La Niña-like state and enhanced Walker circulation (Luo et al., 2012). However, is not yet clear for the past century whether the increase in marine productivity is principally governed by an intensification of the SPSH (Falvey and Garreaud, 2009) or by an enhancement of local winds due to an increase in land-sea thermal gradients caused by anthropogenic greenhouse gas emissions (Bakun, 1990). The OMZ intensity and productivity during the past 100 yr are similar to the pattern observed at the end of the MCA (Fig. 4e, g and h). In both periods the primary productivity shows a declining trend and the export production from higher trophic levels show an increasing trend. Intriguingly, the sediment redox conditions show a trend towards sub-oxic conditions and the OMZ intensity displays a weakening trend, which is in clear contrast to several studies suggesting an expansion of the OMZs under the current global warming (Stramma et al., 2008).

6 Conclusions

Primary productivity, OMZ intensity and sediment redox conditions remained strongly coupled during the last two millennia, and were strongly associated with changes in

ocean-atmosphere systems. This indicate that large scale circulation changes are the driving forces in maintaining productivity and subsurface oxygenation off Peru at centennial time scales during the past two millennia. The observed changes in the PUE are concordant with the "ocean thermostat mechanism" proposed by Clement et al. (1996), suggesting that changes in solar irradiance produce changes in the thermocline depth in the eastern Pacific through changes in the Walker circulation strength. In general, global warm periods are favorable for productivity in the PUE during the last two millennia. Under the current global warming scenario, an SPSH expansion and an intensification of the Walker circulation may likely lead to increased productivity in the PUE.

During the warm periods the SPSH expansion/contraction has more influence over the PUE than the Walker circulation changes. During the MCA, the PUE shows at least two stages in relation to the terrestrial runoff, OMZ intensity, sediment redox conditions, and the different types of export production likely driven by changes in the SPSH expansion/contraction and not by changes in the Walker circulation strength.

The PUE was subject of abrupt as well as gradual changes in OMZ intensity and productivity. The transitions from warm to cold periods shows a gradual change towards lower productivity and less intense OMZ likely linked to the gradual changes in the global temperatures, a gradual weakening of the Walker circulation, and a SPSH contraction. By contrast, the transition of the PUE from the LIA to the CWP, which lasted about 50 yr, was characterized by more abrupt changes as was already shown in previous works.

Supplementary material related to this article is available online at http://www.clim-past-discuss.net/9/5479/2013/cpd-9-5479-2013-supplement.pdf.

Acknowledgements. We deeply thank the Instituto del Mar del Peru (IMARPE) for full support of this research. We acknowledge the crew of the R/V *Jose Olaya Balandra* and all scientific participants in the box-coring survey: E. Enríquez, J. Ledesma, R. Marquina, L. Quipuzcoa,

J. Solis, F. Velazco and L. Vasquez, without their support this research could not have taken place. We acknowledge F. Le Cornec and J. Cottet for their invaluable help with the ICP-Ms analyses. We thank M. Mandeng-Yogo and M. Mendez for the δ^{15}N analyses in the box-core. The AMS radiocarbon measurements were obtained by the "Laboratoire de mesures de C-14" LMC14 (UMS 2572, CEA-CNRS-IRD-IRSN-Ministère de la Culture), Gif-sur Yvette, France, through the IRD financial and technical support to this laboratory. We are grateful to R. Gingold (http://www.sweepandmore.com) for constructive ideas and editing the manuscript. We acknowledge support from the project PALEOMAP, the IAEA Coordinated Research Project 12789 (Nuclear and Isotopic Studies of the El Niño Phenomenon in the Ocean), PALEOTRACES project, PALEOPROXUS project and the *Chaire croisée* PROSUR.

The publication of this article is financed by CNRS-INSU.

References

Aceituno, P., Fuenzalida, R., and Rosenblüth, B.: Climate along the extratropical west coast of South America, in: Earth system responses to global change, edited by: Mooney, H. A., Fuentes, E. R., and Kronberg, B. I., Academic Press, San Diego, 61–69, 1993.

Agnihotri, R., Altabet, M. A., Herbert, T., and Tierney, J. E.: Subdecadally resolved paleoceanography of the Peru margin during the last two millennia, Geochem. Geophy. Geosy., 9, 1–15, 2008.

Altabet, M. A. and Francois, R.: Sedimentary nitrogen isotopic ratio as a recorder for surface ocean nitrate utilization, Global Biogeochem. Cy., 8, 103–116, 1994.

Altabet, M. A., Pilskaln, C., Thunell, R., Pride, C., Sigman, D., Chavez, F., and Francois, R.: The nitrogen isotope biogeochemistry of sinking particles from the margin of the Eastern North Pacific, Deep-Sea Res. Pt. I, 46, 655–679, 1999.

Bakun, A.: Global climate change and intensification of coastal upwelling, Science, 247, 198–201, 1990.

Bertrand, A., Chaigneau, A., Peraltilla, S., Ledesma, J., Graco, M., Monetti, F., and Chavez, F.: Oxygen: A fundamental property regulating pelagic ecosystem structure in the coastal southeastern Tropical Pacific, PLOS ONE, 6, e29558, doi:10.1371/journal.pone.0029558, 2011.

Bird, B. W., Abbott, M. B., Vuille, M., Rodbell, D. T., Stansell, N. D., and Rosenmeier, M. F.: A 2,300-year-long annually resolved record of the South American summer monsoon from the Peruvian Andes, P. Natl. Acad. Sci., 108, 8583–8588, 2011.

Bjerknes, J. H.: Atmospheric teleconnections from the equatorial Pacific, Mon. Weather Rev., 97, 163–172, 1969.

Böning, P., Brumsack, H. J., Bottcher, E., Schnetger, B., Kriete, C., Kallmeyer, J., and Borchers, S. L.: Geochemistry of Peruvian near-surface sediments, Geochim. Cosmochim. Ac., 68, 4429–4451, 2004.

Bradley, R.: 1000 years of climate change, Science, 288, 1353–1355, 2000.

Bradley, R. S., Hughes, M. K., and Diaz, H. F.: Climate in medieval times, Science, 302, 404–405, 2003.

Bratcher, A. J. and Giese, B.S.: Tropical Pacific decadal variability and global warming, Geophys. Res. Lett., 29, 1918, doi:10.1029/2002GL015191, 2002.

Broccoli, A. J., Dahl, K. A., and Stouffer, R. J.: Response of the ITCZ to Northern Hemisphere cooling, Geophys. Res. Lett., 33, L01702, doi:10.1029/2005GL024546, 2006.

Chavez, F. P. and Messié, M.: A comparison of Eastern Boundary Upwelling Ecosystems, Prog. Oceanogr., 83, 80–96, 2009.

Chavez, F. P., Messié, M., and Pennington, J. T.: Marine primary production in relation to climate variability and change, Annu. Rev. Mar. Sci., 3, 227–260, 2011.

Chazen, C. R., Altabet, M. A., and Herbert, T. D.: Abrupt mid-Holocene onset of centennial-scale climate variability on the Peru-Chile margin, Geophys. Res. Lett., 36, L18704, doi:10.1029/2009GL039749, 2009.

Chiang, J. C. H. and Bitz, C. M.: Influence of high latitude ice cover on the marine Intertropical Convergence Zone, Clim. Dynam., 25, 477–496, 2005.

Clement, A. C., Seager, R., Cane, M. A., and Zebiak, S. E.: An Ocean dynamical thermostat, J. Climate, 9, 2190–2196, 1996.

Cobb, K. M., Charles, C. D., Cheng, H., and Edwards, R. L.: El Niño/Southern Oscillation and tropical Pacific climate during the last millennium, Nature, 424, 271–276, 2003.

Colodner, D., Sachs, J., Ravizza, G., Turekian, K., Edmond, J., and Boyle, E.: The geochemical cycle of rhenium: a reconnaissance, Earth Planet. Sc. Lett., 117, 205–221, 1993.
Conroy, J. L., Restrepo, A., Overpeck, J. T., Steinitz-Kannan, M., Cole, J. E., Bush, M. B., and Colinvaux, P. A.: Unprecedent recent warming of surface temperatures in the eastern tropical Pacific Ocean, Nat. Geosci., 2, 46–50, 2009.
Conroy, J. L., Overpeck, J. T., and Cole, J. E.: El Niño/Southern Oscillation and changes in the zonal gradient of tropical Pacific sea surface temperature over the last 1.2 ka, PAGES News, 18, 32–34, 2010.
Crusius, J., Calvert, S., Pedersen, T., and Sage, D.: Rhenium and molybdenum enrichments in sediments as indicators of oxic, suboxic and sulfidic conditions of deposition, Earth Planet. Sc. Lett., 145, 65–78, 1996.
Dean, W. E., Zheng, Y., Ortiz, J. D., and van Geen, A.: Sediment Cd and Mo accumulation in the oxygen-minimum zone off western Baja California linked to global climate over the past 52 kyr, Paleoceanography, 21, PA4209, doi:10.1029/2005PA001239, 2006.
DeMaster, D. J.: The supply and accumulation of silica in the marine environment, Geochim. Cosmochim. Ac., 45, 1715–1732, 1981.
De Pol-Holz, R., Ulloa, O., Dezileau, L., Kaiser, J., Lamy, F., and Hebbeln, D.: Melting of the Patagonian Ice Sheet and deglacial perturbations of the nitrogen cycle in the eastern South Pacific, Geophys. Res. Lett., 33, L04704, doi:10.1029/2005GL024477, 2006.
Diaz-Ochoa, J. A., Lange, C. B., Pantoja, S., De Lange, G. J., Gutierrez, D., Muñoz, P., and Salamanca, M.: Fish scales in sediments from off Callao, central Peru, Deep-Sea Res. Pt. II, 56, 1124–1135, 2008.
Echevin, V., Aumont, O., Ledesma, J., and Flores, G.: The seasonal cycle of surface chlorophyll in the Peruvian upwelling system: A modelling study, Prog. Oceanogr., 79, 167–176, 2008.
Falvey, M. and Garreaud, R. D.: Regional cooling in a warming world: Recent temperature trends in the southeast Pacific and along the west coast of subtropical South America (1979–2006), J. Geophys. Res., 114, D04102, doi:10.1029/2008JD010519, 2009.
Glantz, S. A.: Primer of Biostatistics, McGraw-Hill, 2002.
Graham, N. E., Ammann, C. M., Fleitmann, D., Cobb, K. M., and Luterbacher, J.: Support for global climate reorganization during the "Medieval Climate Anomaly", Clim. Dynam., 37, 1217–1245, 2011.
Gutiérrez, D., Sifeddine, A., Reyss, J. L., Vargas, G., Velazco, F., Salvatteci, R., Ferreira, V., Ortlieb, L., Field, D., Baumgartner, T., Boussafir, M., Boucher, H., Valdés, J., Marinovic, L.,

Soler, P., and Tapia, P.: Anoxic sediments off Central Peru record interannual to multidecadal changes of climate and upwelling ecosystem during the last two centuries, Adv. Geosci., 6, 119–125, doi:10.5194/adgeo-6-119-2006, 2006.
Gutiérrez, D., Sifeddine, A., Field, D. B., Ortlieb, L., Vargas, G., Chávez, F. P., Velazco, F., Ferreira, V., Tapia, P., Salvatteci, R., Boucher, H., Morales, M. C., Valdés, J., Reyss, J.-L., Campusano, A., Boussafir, M., Mandeng-Yogo, M., García, M., and Baumgartner, T.: Rapid reorganization in ocean biogeochemistry off Peru towards the end of the Little Ice Age, Biogeosciences, 6, 835–848, doi:10.5194/bg-6-835-2009, 2009.
Gutiérrez, D., Bouloubassi, I., Sifeddine, A., Purca, S., Goubanova, K., Graco, M., Field, D., Méjanelle, L., Velazco, F., Lorre, A., Salvatteci, R., Quispe, D., Vargas, G., Dewitte, B., and Ortlieb, L.: Coastal cooling and increased productivity in the main upwelling zone off Peru since the mid-twentieth century, Geophys. Res. Lett., 38, L07603, doi:10.1029/2010GL046324, 2011.
Haug, G. H., Hughen, K. A., Sigman, D. M., Peterson, L. C., and Rohl, U.: Southward migration of the Intertropical Convergence Zone through the Holocene, Science, 293, 1304–1308, 2001.
Helly, J. and Levin, L.: Global distribution of naturally occurring marine hypoxia on continental margin, Deep-Sea Res. Pt. I, 51, 1159–1168, 2004.
Karstensen, J. and Ulloa, O.: Peru-Chile current system, in: Ocean currents, edited by: Steele, J. H., Thorpe, S. A., and Turekian, K. K., Academic Press, 2009.
Kienast, M., Kienast, S. S., Calvert S. E., Eglinton, T. I., Mollenhauer G., François, R., and Mix, A. C.: Eastern Pacific cooling and Atlantic overturning circulation during the last deglaciation, Nature, 443, 846–849, 2006.
Koffman, B. G., Kreutz, K. J., Breton, D. J., Kane, E. J., Winski, D. A., Birkel, S. D., Kurbatov, A. V., and Handley, M. J.: Centennial-scale shifts in the position of the Southern Hemisphere westerly wind belt over the past millennium, Clim. Past Discuss., 9, 3125–3174, doi:10.5194/cpd-9-3125-2013, 2013.
Koutavas, A. and Lynch-Stieglitz, J.: Variability of the marine ITCZ over the eastern Pacific during the past 30,000 years, in: The Hadley circulation: present, past and future, edited by: Diaz, E. F. and Bradley, R. S., Springer Academic Publishers, 2005.
Koutavas, A., Lynch-Stieglitz, J., Marchitto, T. M., and Sachs, J. P.: El Niño-like pattern in ice age tropical Pacific sea surface temperature, Science, 297, 226–230, 2002.
Lamb, H. H.: Climate, History and the Modern World, Routledge, New York, 2nd edition, 1995.

Lamy, F., Hebbeln, D., Röhl, U., and Wefer, G.: Holocene rainfall variability in southern Chile: a marine record of latitudinal shifts of the Southern Westerlies, Earth Planet. Sc. Lett., 185, 369–382, 2001.
Lee, S. and Feldstein, S. B.: Detecting ozone- and greenhouse gas-driven wind trends with observational data, Science, 339, 563–567, 2013.
Luo, J.-J., Sasaki, W., and Masumoto, Y.: Indian Ocean warming modulates Pacific climate change, P. Natl. Acad. Sci., 109, 18701–18706, 2012.
Makou, M. C., Eglinton, T. I., Oppo, D. W., and Hughen, K. A.: Postglacial changes in El Niño and La Niña behavior, Geology, 38, 43–46, 2010.
Mann, M. E., Cane, M. A., Zebiak, S. E., and Clement, A.: Volcanic and solar forcing of the Tropical Pacific over the past 1000 years, J. Climate, 18, 447–456, 2005.
Mann, M. E., Zhang, Z., Rutherford, S., Bradley, R. S., Hughes, M. K., Shindell, D., Ammann, C., Faluvegi, G., and Ni, F.: Global signatures and dynamical origins of the Little Ice Age and Medieval Climate Anomaly, Science, 326, 1256–1260, 2009.
Martinez, P. and Robinson, R. S.: Increase in water column denitrification during the last deglaciation: the influence of oxygen demand in the eastern equatorial Pacific, Biogeosciences, 7, 1–9, doi:10.5194/bg-7-1-2010, 2010.
McManus, J., Berelson, W. M., Severmann, S., Poulson, R. L., Hammond, D. E., Klinkhammer, G. P., and Holm, C.: Molybdenum and uranium geochemistry in continental margin sediments: Paleoproxy potential, Geochim. Cosmochim. Ac., 70, 4643–4662, 2006.
Michaels, A. F. and Silver, M. W.: Primary production, sinking fluxes and the microbial food web, Deep-Sea Res. Pt. IA, 35, 473–490, 1988.
Mohtadi, M., Romero, O., Kaiser, J., and Hebbeln, D.: Cooling of the southern high latitudes during the Medieval Period and its effect on ENSO, Quaternary Sci. Rev., 26, 1055–1066, 2007.
Mollier-Vogel, E., Ryabenko, E., Martinez, P., Wallace, D., Altabet, M. A., and Schneider, R.: Nitrogen isotope gradients off Peru and Ecuador related to upwelling, productivity, nutrient uptake and oxygen deficiency, Deep-Sea Res. Pt. I, 70, 14–25, 2012.
Montes, I., Colas, F., Capet, X., and Schneider, W.: On the pathways of the equatorial subsurface currents in the eastern equatorial Pacific and their contributions to the Peru-Chile Undercurrent, J. Geophys. Res., 115, C09003, doi:10.1029/2009JC005710, 2010.
Moy, C. M., Moreno, P. I., Dunbar, R. B., Kaplan, M. R., Francois, J.-P., Villalba, R., and Haberzettl, T.: Climate change in southern South America during the last two millennia, in:

Past climate variability in South America and surrounding regions, edited by: Vimeaux, F., Springer, Netherlands, 2009.
Nameroff, T. J., Calvert, S. E., and Murray, J. W.: Glacial-interglacial variability in the eastern tropical North Pacific oxygen minimum zone recorded by redox-sensitive trace metals, Paleoceanography, 19, PA1010, doi:10.1029/2003PA000912, 2004.
Oppo, D. W., Rosenthal, Y., and Linsley, B. K.: 2,000-year-long temperature and hydrology reconstructions from the Indo-Pacific warm pool, Nature, 460, 1113–1116, 2009.
PAGES 2K Network. Continental-scale temperature variability during the past two millennia, Nat. Geosci., 6, 339–346, 2013.
Partin, J. W., Cobb, K. M., Adkins, J. F., Clark, B., and Fernandez, D. P.: Millennial-scale trends in west Pacific warm pool hydrology since the Last Glacial Maximum, Nature, 449, 452–455, 2007.
Pennington, J. T., Mahoney, K. L., Kuwahara, V. S., Kolber, D. D., Calienes, R., and Chavez, F. P.: Primary production in the eastern tropical Pacific: A review, Prog. Oceanogr., 69, 285–317, 2006.
Philander, S. G.: El Niño, La Niña, and the Southern Oscillation, Academic Press, 1990.
Pierrehumbert, R. T.: Climate change and the tropical Pacific: The sleeping dragon wakes, P. Natl. Acad. Sci., 97, 1355–1358, 2000.
Rein, B., Lückge, A., and Sirocko, F.: A major Holocene ENSO anomaly during the Medieval period, Geophys. Res. Lett., 31, L17211, doi:10.1029/2004GL020161, 2004.
Rein, B., Lückge, A., Reinhardt, L., Sirocko, F., Wolfe, A., and Dullo, W.-C.: El Niño variability off Peru during the last 20,000 years, Paleoceanography, 20, PA4003, doi:10.1029/2004PA001099, 2005.
Reinhardt, L., Kudrasss, H.-R., Lückge, A., Wiedicke, M., Wunderlich, J., and Wendt, G.: High-resolution sediment echosounding off Peru: Late Quaternary depositional sequences and sedimentary structures of a current-dominated shelf, Mar. Geophys. Res., 23, 335–351, 2002.
Reuter, J., Stott, L., Khider, D., Sinha, A., Cheng, H., and Edwards, R. L.: A new perspective on the hydroclimate variability in northern South America during the Little Ice Age, Geophys. Res. Lett., 36, L21706, doi:10.1029/2009GL041051, 2009.
Robinson, R., Kienast, M., Albuquerque, A. S., Altabet, M. A., Contreras, S., De Pol-Holz, R., Dubois, N., Francois, R., Galbraith, E. D., Hsu, T.-C., Ivanochko, T. S., Jaccard, S. L., Kao, S.-J., Kiefer, T., Kienast, S., Lehmann, M., Martinez, P., McCarthy, M., Möbius, J. H., Ped-

ersen, T. F., Quan, T. M., Ryabenko, E., Schmittner, A., Schneider, R., Schneider-Mor, A., Shigemitsu, M., Sinclair, D., Somes, C. J, Studer, A. S., Thunell, R., and Yang, J.-Y. T.: A review of nitrogen isotopic alteration in marine sediments, Paleoceanography, 27, PA4203, doi:10.1098/rsta.2012.0396, 2012.

Rodier, M. and Le Borgne, R.: Export flux of particles at the equator in the western and central Pacific ocean, Deep-Sea Res. Pt. II, 44, 2085–2113, 1997.

Sachs, J. P., Sachse, D., Smittenberg, R. H., Zhang, Z., Battisti, D. S., and Golubic, S.: Southward movement of the Pacific Intertropical Convergence Zone AD 1400–1850, Nat. Geosci., 2, 519–525, 2009.

Salvatteci, R., Field, D., Sifeddine, A., Ortlieb, L., Ferreira, V., Baumgartner, T., Caquineau, S., Velazco, F., Reyss, J. L., Sanchez-Cabeza, J. A., and Gutierrez, D.: Cross-stratigraphies from a seismically active mud lens off Peru indicate horizontal extensions of laminae, missing sequences, and a need for multiple cores for high resolution records, Mar. Geol., in review, 2013.

Scheidegger, K. F. and Krissek, L. A.: Dispersal and deposition of eolian and fluvial sediments off Peru and northern Chile, Geol. Soc. Am. Bull., 93, 150–162, 1982.

Sifeddine, A., Gutierrez, D., Ortlieb, L., Boucher, H., Velazco, F., Field, D., Vargas, G., Boussafir, M., Salvatteci, R., Ferreira, V., García, M., Valdes, J., Caquineau, S., Mandeng-Yogo, M., Cetin, F., Solis, J., Soler, P., and Baumgartner, T.: Laminated sediments from the central Peruvian continental slope: A 500 year record of upwelling system productivity, terrestrial runoff and redox conditions, Prog. Oceanogr., 79, 190–197, 2008.

StatSoft, Inc. STATISTICA (data analysis software system), Version 7.1., http://www.statsoft.com, 2005.

Stramma, L., Johnson, G. C., Sprintall, J., and Mohrholz, V: Expanding Oxygen-Minimum Zones in the Tropical Oceans, Science, 320, 655–658, 2008.

Stramma, L., Schmidtko, S., Levin, L. A., and Johnson, G. C.: Ocean oxygen minima expansions and their biological impacts, Deep-Sea Res. Pt. I, 57, 587–595, 2010.

Strub, P. T., Mesias, J. M., Montecino, V., Rutllant, J., and Salinas, S.: Coastal ocean circulation off western South America, in: The Sea, Vol.11, edited by: Robinson, A. and Brink, K., John Wiley & Sons , New York, USA, 273–313, 1998.

Suess, E.: Particulate organic carbon flux in the oceans-surface productivity and oxygen utilization, Nature, 288, 260–263, 1980.

Tribovillard, N., Algeo, T. J., Lyons, T., and Riboulleau, A.: Trace metals as paleoredox and paleoproductivity proxies: An update, Chem. Geol., 232, 12–32, 2006.

Vecchi, G. A., Soden, B., Wittenberg, A. T., Held, I. M., Leetmaa, A., and Harrison, M. J.: Weakening of tropical Pacific atmospheric circulation due to anthropogenic forcing, Nature, 44, 73–76, 2006.

Yan, H., Sun, L., Wang, Y., Huang, W., Qiu, S., and Yang, C.: A record of the Southern Oscillation Index for the past 2,000 years from precipitation proxies, Nat. Geosci., 4, 611–614, 2011.

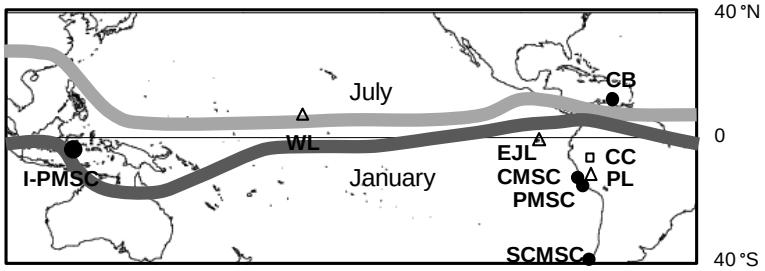

Fig. 1. Map showing modern locations of the ITCZ in July and January, modified from Newton et al. (2006), and the localities discussed in the text: I-PMSC, Indo-Pacific Marine sediment core (Oppo et al., 2009); WL, Washington Lake (Sachs et al., 2009); CB, Cariaco Basin (Haug et al., 2001); EJL, El Junco lake (Conroy et al., 2009); CC, Cascayunga cave (Reuter et al., 2009); PL, Pumacocha lake (Bird et al., 2011); CMSC, Callao marine sediment core (Rein et al., 2005); PMSC, Pisco marine sediment cores (the present study); SCMSC, Southern Chile marine sediment core (Lamy et al., 2001). The circles indicate the marine sediment cores, the square indicates the speleothem, and the triangles indicate the lake sediment cores. Coastline contours obtained from "Coastline Extractor" available at: http://www.ngdc.noaa.gov/mgg/coast/.

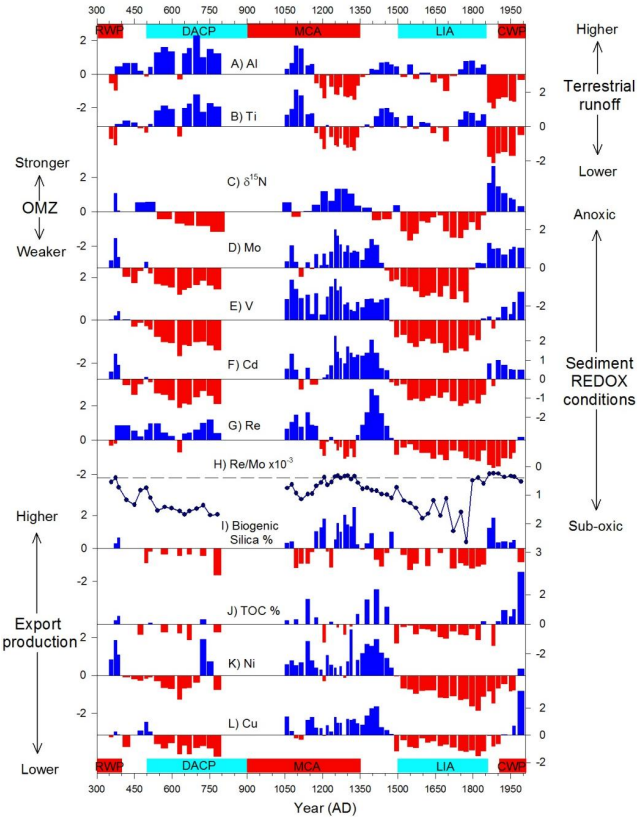

Fig. 2. Standardized values (value-average) / sd) of the proxies evaluated in the present study. **(A)** Aluminum (Al) proxy for terrestrial runoff. **(B)** Titanium (Ti) proxy for terrestrial runoff. **(C)** δ^{15}N, proxy for water column denitrification. **(D)**, **(E)**, **(F)** and **(G)** Molybdenum (Mo), Vanadium (V), Cadmium (Cd) and Rhenium (Re), proxies for sediment redox conditions. **(H)** Ratio $Re/Mo \times 10^{-3}$, proxy to differentiate anoxic versus sub-oxic conditions, the dashed line indicates the seawater value of $Re/Mo = 0.4 \times 10^{-3}$ reported by Crusius et al. (1996). **(I)** Biogenic silica (%), proxy for siliceous export production. **(J, K, L)** Total organic carbon (TOC), Nickel (Ni) and Copper (Cu) export production proxies. The colored boxes at the top and bottom of the figure indicate the Roman Warm Period (RWP), the Dark Ages Cold Period (DACP), the Medieval Climate Anomaly (MCA), the Little Ice Age (LIA) and the Current Warm Period (CWP). The data corresponding to the LIA and CWP were lumped into intervals of ~ 20 yr to fit the sample resolution of the older periods. Note that in this figure, Cd is used to represent sediment redox conditions while in Fig. 3 this metal is presented as an export production proxy, see text for detailed information.

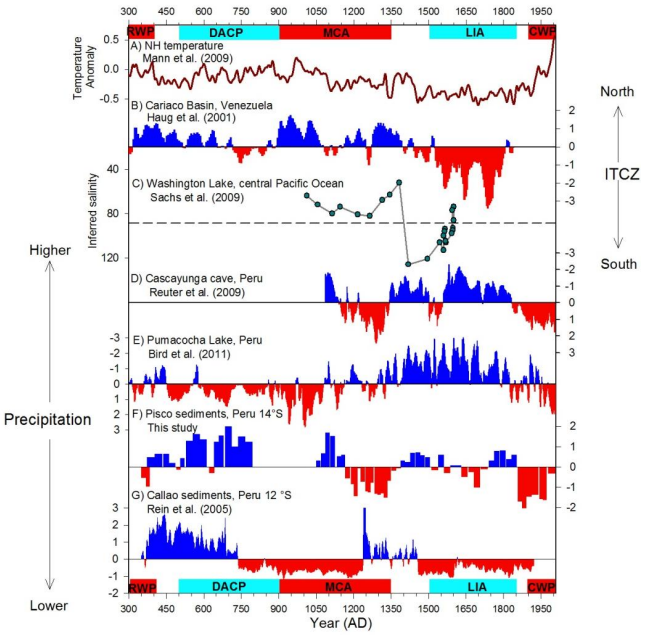

Fig. 3. Precipitation proxies during the last 2 millennia and selected records from the literature. **(A)** 10-point average of the northern hemisphere (NH) temperature anomaly (Mann et al., 2009), **(B)** 3-point average of Ti% in Cariaco Basin (Haug et al., 2001), **(C)** Inferred salinity in Washington Island lake (Sachs et al., 2009), **(D)** 5-point average of Cascayunga cave speleothem rainfall δ^{18}O (Reuter et al., 2009), **(E)** 5-point average Pumacocha $\delta^{18}O_{cal}$ record (Bird et al., 2011), **F)** Al content in the present study, **(G)** A proxy for lithic concentration in a marine sediment core retrieved off Callao (~ 12 ° S) (Rein et al., 2005). The series were smoothed using a running mean when indicated and then normalized to a standard Z-score. The colored boxes at the top and bottom of the figure indicate the Roman Warm Period (RWP), the Dark Ages Cold Period (DACP), the Medieval Climate Anomaly (MCA), the Little Ice Age (LIA) and the Current Warm Period (CWP).

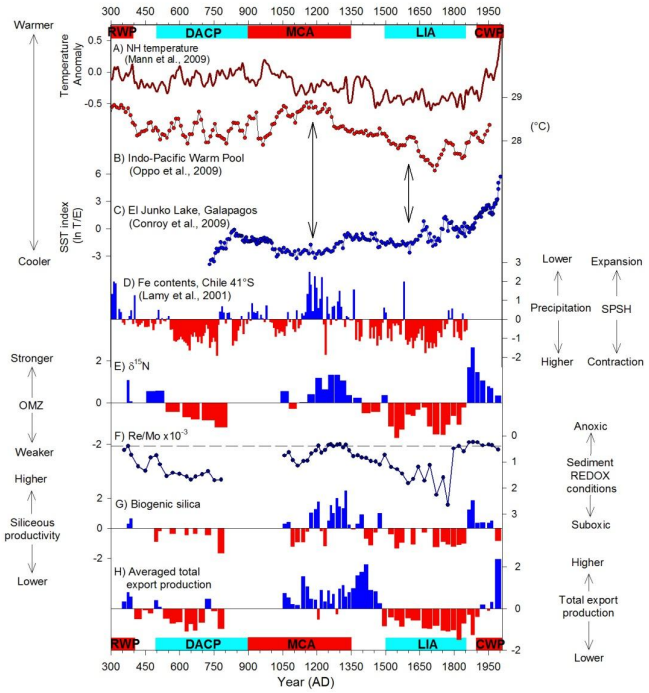

Fig. 4. Linkage between the oxygenation in the subsurface waters and in the sediments, and the export production obtained in the present work and proxies used to infer changes in the zonal SST gradients and changes in the expansion/contraction of the South Pacific Sub Tropical High (SPSH). **(A)** 10-point average of the northern hemisphere (NH) temperature anomaly (Mann et al., 2009). **(B)** Indo Pacific Warm Pool SST reconstruction (Oppo et al., 2009). **(C)** Eastern Equatorial Pacific SST reconstruction (ln of the number of tychoplanktonic to epiphytic diatoms in El Junco Lake, Galapagos, Conroy et al., 2009).The arrows between these two panels show the increased SST gradient during the MCA compared to the LIA (Conroy et al., 2010). **(D)** 3-point average of Fe intensity in a marine sediment core off Chile ($\sim 41^{\circ}$ S), where lower (higher) values indicate a more poleward (equatorward) position of the westerlies and thus an expansion (contraction) of the SPSH. Relative low iron contents are related to enhanced runoff from the iron-poor coastal ranges when the westerlies were positioned over the core position (Lamy et al., 2001), consequently lower Fe values indicate higher precipitation, and thus a more equatorward position of the southern westerlies and the south rim of the SPSH. **(E)** δ^{15}N, proxy for water column denitrification. **(F)** Ratio $\mathrm{Re}/\mathrm{Mo} \times 10^{-3}$, proxy to differentiate anoxic versus sub-oxic conditions, the dashed line indicates the seawater value of $\mathrm{Re}/\mathrm{Mo} = 0.4 \times 10^{-3}$ reported by Crusius et al. (1996). **(G)** Biogenic silica (%), proxy for siliceous export production. **(H)** Averaged total export production obtained from the standardized TOC, Ni and Cu values. The colored boxes at the top and bottom of the figure indicate the Roman Warm Period (RWP), the Dark Ages Cold Period (DACP), the Medieval Climate Anomaly (MCA), the Little Ice Age (LIA) and the Current Warm Period (CWP).